Fall transition drives declines in densities and shifts in distribution of zooplankton and marine bird taxa in the San Juan Islands

Timothy Glenn P. Iringan

Pelagic Ecosystem Function 2024

Timothy Glenn P. Iringan
Friday Harbor Laboratories, University of Washington, Friday Harbor, WA 98250
tgpiringan@gmail.com

Keywords: *fall transition, species distribution, marine bird, zooplankton, San Juan Island, generalized additive model, Larus glaucescens, Uria aalge, copepod, amphipod*

Abstract

Numerous ocean and biological monitoring programs present in the San Juan Archipelago (SJA) allow for regional-scale correlations of ocean factors to near end-member trophic level representatives for an ecosystem perspective on seasonal climate shifts. This study investigates population density and density distribution variations of two marine bird and two zooplankton taxa as a function of several environmental drivers around the time period of the fall transition, an annual climatic shift of prevailing winds and accompanying physical and chemical oceanographic changes. Generalized additive models (GAM) were used to define possible nonlinear relationships and to determine the relative contributions of each environmental driver to taxon density. The GAM results were then used to predict density distributions over San Juan Archipelago. Common murre (*Uria aalge*), copepod, and amphipod high-density areas were predicted to be significantly reduced after the fall transition with 63%, 71%, and 71% reductions, respectively, relative to before the fall transition. Glaucous-winged gulls (*Larus glaucescens*) were not significantly impacted by this seasonal change and maintained their high-density areas throughout the fall transition. Sea surface temperature was found to be the most significant factor on all affected taxa, followed by mixing for zooplankton. Total abundance was not significantly different for common murres and copepods before and after the fall transition while amphipod abundance dropped after the fall transition, meaning that the decline in high-density areas for the murres and copepods were a result of a more even distribution of the population across SJA while amphipod densities decreased as a function of lower overall abundance. Identifying the tolerance of these taxa to environmental features gives insight on how their distribution might change in future climate scenarios and on conservation efforts of more economically important species that are directly related to these taxa.

1. Introduction

One of the many challenges in ecological studies lie in achieving real-world applicability by considering multiple drivers over extended ranges of time and space. Efforts to achieve this are hampered both by practicality and by the reduction of the experimental design to produce intuitive and mechanistic results (Boyd et al., 2018). Time series datasets such as those in the San Juan Archipelago (SJA) provide an opportunity to bypass this limitation and allow for seasonal and regional scale population distribution assessment of key members in the ecosystem in response to contemporaneously measured physical factors. There is a continuing community effort on biodiversity conservation in the SJA which includes the establishment and maintenance of biological preserves, marine protected areas, wildlife refuge, and fish recovery zones (Don, 2002; Evans &

Kennedy, 2007). Understanding how to manage these sanctuaries requires comprehensive knowledge on the natural and anthropogenic pressures that act upon them.

Among those natural pressures are seasonal progressions associated with temperate latitudes. The fall transition is an annual climatological shift of prevailing wind direction and intensity from strong northerly summer winds to weak southerly winds along the US Pacific coast that occurs at some point in September or October (Bakun & Nelson, 1991). This shift is accompanied by changes in other factors such as wind-driven surface currents, sea surface temperature (SST), salinity, rainfall, and upwelling intensity. While its effects on the physical and chemical ocean are relatively well known, the ecological response to the fall transition, particularly in relation to congregation patterns and habitat use, is still relatively unknown.

Previous studies have mapped distributions of certain groups of marine birds and mammals to inform conservation efforts (Cox, 2021; Gillman, 2021). Resident mammals that serve as sentinel species such as pinnipeds and cetaceans are conspicuous but are rarer to find and subsequently map. Some marine birds, in contrast, are present throughout the year (Blight et al., 2015; Reid, 1988) with markedly greater abundances which makes them relatively easier to observe. Monitoring the behavior of these predators provides a top-down insight into the marine ecosystem of the Salish Sea.

Two bird species are of interest in this study. Glaucous-winged gulls (*Larus glaucescens*) are nearshore non-diving birds which prey on intertidal invertebrate communities and pelagic fishes (Domalik et al., 2021; Irons et al., 1986). A time series analysis of the population of glaucous-winged gulls in the greater Salish Sea showed a steady population decline since the late 1980s (Blight et al., 2015), which reflects their sensitivity to changing ecological and environmental conditions. Common murres (*Uria aalge*) are diving birds whose diet consists of small forage fishes and squid (Ainley et al., 1996). Migratory tracking of these birds shows foraging in different water mass types at different phenological stages (Loredo, 2018). In addition to their own roles as top predators, both groups show potential as indicator species for environmental monitoring.

Zooplankton represent the lowest trophic level in the marine ecosystem that is not traditionally remotely sensed as compared to phytoplankton. This group provides a vital link between primary productivity and higher trophic levels and constitutes a significant portion of the carbon cycle (Steinberg et al., 2000). Biomass trends of over two decades of the Strait of Georgia zooplankton community are reported to decrease with increasing salinity (Perry et al., 2021), which may underlie a reliance on certain water masses. Alongside phytoplankton proxies, zooplankton provide a view of the ecological system from a bottom-up standpoint.

In this study, the ecosystem response to the fall transition is investigated from diametrically opposed ecological viewpoints: marine birds and zooplankton. Density models are calculated for two marine bird and two zooplankton taxa as a function of environmental and geographic variables using generalized additive models (GAM) built upon an observational time series in the San Juan Channel. These are then used to construct species distribution models (SDM) for SJA before and after the fall transition to determine how the progression of the season affects the habitat suitability of SJA for these groups in the form of density predictions.

To achieve this, we introduce the term 'aggregation zone', which will be an object of comparison for this study. These are unit areas with a population density above a certain threshold, calculated from the overall density distribution around the fall transition (see 2.6), and are grouped together by their position relative to the fall transition (before or after), to see how they are temporally and spatially distributed in SJA. The fall transition is broken down to its climatic components: SST, surface salinity, temperature standard deviation (TSD), wind intensity, and primary productivity as represented by phytoplankton biomass. The standard deviation of temperature represents the variance of SST in a given area and is also a proxy for water fronts (Cox, 2021). Geographic factors such as bathymetry, depth gradient, and distance from the shore are added in to account for the complex interactions between ocean parameters and the archipelagic setting.

2. Methods

2.1. Geographic setting

The San Juan Archipelago is located in the Salish Sea, an estuarine fjord, between mainland Washington and the US-Canada border (fig 1). River input comes mainly from the Fraser River in the north with peak discharge during summer and a smaller peak during the start of storm season in November, driving estuarine circulation year round with seasonal intensities (Pawlowicz et al., 2007; Rapaport, 2024; Sutherland et al., 2011). The southern end of San Juan Channel typically experiences more marine conditions due to its proximity to Haro Strait, and the shallow sill near Cattle Point causes gravity-induced turbulent mixing on the flood side (Thomson et al., 2020; Zamon, 2003). The study area includes all major islands of San Juan County (latitude limits: 48.40°, 48.73°, longitude limits: -123.22°, -122.72°). All GIS analyses were done in MATLAB 2023b using the Mapping Toolbox (The MathWorks Inc., 2024).

2.2. Field survey

Annual oceanographic and marine bird surveys are conducted along the San Juan Channel by the Pelagic Ecosystem Function (PEF) course of Friday Harbor Laboratories (FHL), University of Washington. Several weekly surveys are done in the autumn around the time of the fall transition using the same stations and transects each time (Table 1) aboard the *R/V Rachel Carson* or *R/V Kittiwake*. A CTD cast (SBE 19plus V2 SeaCAT Profiler CTD; SBE 911plus CTD, Sea-Bird Scientific) is deployed each for North and South stations (table 1) to characterize water column conditions at the time of sampling. The CTD profiler is attached to a Niskin rosette that collects discrete water samples at different depths. Seawater for each Niskin depth were transferred into opaque 250 mL bottles for chlorophyll-a analysis. These bottles were rinsed thrice with sample water before filling them to the brim and storing them in a cooler.

Vertical zooplankton tows (mesh size = 153 μm, ring diameter = 0.7m) with a TSK 2273 flowmeter were also cast on the entire water column of both stations for density measurements. Oblique tows due to currents were corrected for by determining an adjusted length of tow line based on the tow angle. Upon retrieval, the mesh net was rinsed from the outside with seawater to guide any zooplankton attached to the net into the cod end. Samples were then transferred to jars and were preserved with 60 mL of formalin for a final concentration of ~5% formalin.

The marine bird survey transect is divided into six zones based on geographic factors such as channel width, bathymetry, transect orientation, and the presence of a confluence. Paired observers, one each for port and starboard sides of the research vessel, log the number of bird taxa spotted by the minute per zone within an approximate 200-m radius. Observations were done twice per zone as the vessel goes from North to South station and back again over the course of the day. These were averaged to minimize tidal influence.

2.3. Environmental data

Gridded model values for four dynamic variables (SST, salinity, phytoplankton, and wind intensity) of the San Juan Archipelago were obtained from LiveOcean (MacCready et al., 2021) for years 2017 to 2023 with a daily temporal resolution and a 500-m spatial resolution. Contained within the defined map quadrangle is a 73-by-74 latitude-longitude grid of LiveOcean data points. Polygons were then constructed to represent each zone (fig 1). To adjust for the coarser spatial resolution of the model, the polygons have a 500-m width on each side of the transect line instead of 200-m as in the visual survey. Points in the gridded data that fall on or within the polygon will be averaged to get the value for that zone. This is done for all zones in PEF cruise dates within the year range of the

dataset. Temperature and salinity are diagnostic parameters for water mass identification and the chlorophyll-phytoplankton parameters are indicative of primary productivity. Wind intensity is a parameter related to surface currents and mixed layer mixing intensity. Another variable, the temperature standard deviation (TSD), is added in to represent water mass fronts (Cox, 2021).

Three static variables, depth, topography, and distance from shore, were also added in as factors based on a previous study (Cox, 2021), with slight modifications: channel width was omitted as some grid points fall into open ocean areas and the static tidal current amplitude was replaced by the dynamic variable wind speed. Depth alludes to the possibility of different water masses existing in the water column and the interactions among them while topography is the roughness of the bathymetry in a given area. Steep gradients in topography may have effects in turbulence and mixing. Distance from shore is added in to account for the tendency of birds to hunt nearshore (Domalik et al., 2021). Bathymetry data was obtained from the U.S. Coastal Relief Model (Vol.8, Northwest Pacific) (NOAA National Geophysical Data Center, 2003). Depth and topography for each zone were calculated in the same way as the dynamic variables using the mean and the standard deviation of the bathymetry data, respectively. Distance from shore was obtained by computing the distance of each zone's midpoint to all points in the SJA shapefile and identifying the minimum value.

2.4. Lab analysis

Zooplankton tow samples were filtered in a 118-µm mesh sieve and rinsed with tap water. Large taxa such as hydrozoan medusae were removed and recorded before progressively splitting the remaining zooplankton in halves using a Folsom plankton splitter until a suitable amount for counting of about 200-300 taxa is achieved. The fraction used in counting was transferred to a graduated cylinder and left to settle for five minutes. The settled zooplankton and the diluted volumes were recorded before transferring the fraction into a jar and obtaining two 5-mL aliquots from it using a Hensel-Stempel pipette. These aliquots were transferred to acrylic counting chambers and taxon abundances were tallied using a Nikon SMZ645 dissecting microscope. Taxon densities were calculated using Equation 1,

$$d_T = \frac{x \cdot \frac{V_d}{V_a} \cdot \frac{1}{F}}{V_{tow}} \quad (1)$$

where d_T is the density per taxon, x is the taxon abundance in an aliquot, V_d is the diluted volume, V_a is the aliquot volume, F is the Folsom split factor (e.g.., a quarter split is equal to 0.25), and V_{tow} is the volume of towed water as calculated from the flow meter and ring net diameter. Mean density was obtained by averaging the two aliquot taxon densities.

Chlorophyll-a was measured spectrophotometrically using a Turner Designs Trilogy Laboratory fluorometer. The particulate fraction of each sample was collected by filtering the sample through a 25 mm 0.7 μm glass microfiber filter. The filters were folded, placed into test tubes with 10 mL 90% acetone, and were left overnight in the freezer. They were then placed into glass cuvettes and were measured using the chlorophyll-a acid module of the fluorometer. Surface depths were measured in duplicates.

2.5. Data validation

Calibration of the LiveOcean dataset was done prior to computations to match *in situ* observations. Model values for sea surface temperature, salinity, and phytoplankton were compared to CTD-derived SST and salinity, and surface-sampled chlorophyll, respectively, for all zones during cruise dates. Calibration was done using linear regression. For each variable, yearly data that grossly deviated from the fitted line and were well outside the cloud of the remaining points were removed. Collinearity of predictors were assessed by constructing a correlation matrix and one member of a paired correlation with an R-squared value of 0.5 is removed.

2.6. GAM and SDM generation

Generation of GAMs was done in R version 4.4.1 under the *mgcv* package (R Core Team, 2024; Wood, 2011). Bird GAMs included both dynamic and static variables as predictors while zooplankton GAMs only included dynamic variables as they only have two stations, and therefore only two x-axis points, that would not be advisable to put into the GAM. The number of knots for dynamic and static variables were set to four and three respectively to avoid overfitting. Automatic selection of variables with significant effects to the taxa density was enabled when running the *gam* function as it was tested to return the best possible combination of variables for the model (M. Sigler et al., 2023).

A subset of the observations of glaucous-winged gulls and common murres were taken to confirm the validity of the constructed GAMs while the whole of the zooplankton dataset was devoted to model training as it only had 56 observations. Twenty percent of the total observations were randomly selected and withheld from model calculations for testing. The test subsets were divided by zone (n = 6-10) and were used to compute for predicted densities for the two bird taxa. The predicted values were then compared to the observed values using a paired *t*-test to examine the validity of the constructed GAMs.

To construct distribution models for before and after the fall transition, the estimated transition date is derived from a 10-day running mean of the Coastal Upwelling Transport Index

(previously the Bakun Upwelling Index) (Jacox et al., 2018), with transition date selected as the first Julian day followed by consistent negative values. Fourteen days before and after the identified fall transition dates were noted and LiveOcean data for those dates were compiled and refitted into 1-km grids by averaging 3-by-3 squares. The LiveOcean spatial data are calibrated to *in situ* data and represent pre- and post-transition conditions which were used as factors for the SDMs.

The last step was to identify aggregation zones for the marine birds. The area of 1-km^2 units above the 90th percentile, hereafter termed an aggregation zone, was recorded for each date and the average for each group were compared in a *t*-test to determine whether bird densities within the aggregation zones had changed between the two time periods (i.e., before and after the fall transition).

3. Results

3.1. Ocean model calibration and correlation of dynamic variables

There is a general agreement between CTD or Niskin bottle data and the modeled LiveOcean dataset (table 2), especially for SST which had a near-zero intercept and a near-one slope. Much less can be said for salinity. Although correlation is still high, points start to become more scattered in low salinities, indicating that the model has much less prediction power for fresher conditions, with a lower limit of 10.52 psu (y-intercept).

Of the five dynamic variables employed, two pairwise regressions returned an R-squared value greater than 0.50: phytoplankton-SST (R^2 = 0.53) and phytoplankton-temperature standard deviation (TSD) (R^2 = 0.86) (fig 3). Highly collinear pairs such as these should be addressed in the GAMs to avoid redundancy in variables that behave similarly to each other. Since the common variable for both pairs is phytoplankton, it was omitted in the GAMs. Additionally, the low R-squared value for the SST-salinity pair (R^2 = 0.15) may be due to the presence of several water masses in the transect area alone, such as freshwater pulse events by the Fraser River from the north.

3.2. Pre- and post- fall transition ocean conditions

Ocean conditions before and after the fall transition from 2017 to 2023 were compared by randomly selecting approximately 250 points across space and time for each group and comparing them for SST, salinity, TSD, and wind intensity. All four factors significantly changed in the 28-day window around the fall transition ($p < 0.0001$) (fig 4, table3) with mean differences of −1.1°C for SST, 1 PSU for salinity, −0.02°C for temperature std dev, and 0.65 m/s for wind intensity.

3.3. Test subset

Paired *t*-tests for zones showed no significant differences between the observed and predicted densities of glaucous-winged gulls and common murres except for zone 5 for the gulls and zones 5 and 6 for the murres where there was a noticeable difference in mean density, albeit with non-significant *p*-values (fig 5, table 4). Predicted values for the glaucous-winged gull show less variance while the common murre variances remain the same for both predicted and observed sets, alluding to a slightly better performance of the model for the murres.

3.4. Generalized additive models

Automatic selection in the *gam* function determined all predictor variables were significant except SST for glaucous-winged gull (fig 6-9). For the rest of the taxa, density is shown to increase with temperature. In contrast, salinity does not have any major impact in terms of magnitude on the birds. For zooplankton, the salinity plot shows a mid-salinity peak in density (fig 8-9). The negative slope of this salinity relationship for zooplankton is associated with the densely grouped data points and is consistent with previous findings (Perry et al., 2021). For the TSD, there is a general decreasing trend in density as temperature variance increases for common murres and amphipods. This trend for the common murre is also consistent with previous findings (Cox, 2021). Glaucous-winged gulls have a local density maximum in the middle of the TSD range while copepods have a middle density minimum. There is also a density minimum for birds with regards to wind at approximately 2.5-3 ms^{-1}, while zooplankton shows decreasing density with increasing wind speed.

For the static variables, the two bird groups experience contrasting behaviors with respect to depth, wherein glaucous-winged gulls tend to populate shallower areas while common murres are denser toward deeper waters. Topography shows an unexpected trend where there is decreased densities in steeper or rougher bathymetry while distance from shore plots show maxima for both birds in mid-range distances (1-1.2 km).

Based on chi-square results for each predictor (table 5), wind intensity and distance from shore are the most influential factors for glaucous-winged gulls while SST is the most influential factor for common murres, closely followed also by distance from shore. For the zooplankton, TSD and wind intensity explain the most variance in copepod density while SST and TSD do for amphipods.

3.5. Species distribution models

All groups had diminished aggregation zones post-fall transition, with all but the glaucous-winged gull being statistically significant (fig 10, table 6). Similarly, all but the gulls have much less

density variances after the fall transition. Of the four taxa, gulls have the most resistance to changes in ocean conditions and are more reliant to geographic variables. As a result, gull distribution has been consistent throughout all the days of both before and after groups with a strong fidelity to nearshore waters (fig 11). Murres also have a strong affinity to nearshore areas but are more reactive to changes in temperature (fig 12). Marginally higher densities of murres can be found whenever pulses of warm estuarine waters invade the study area from the north. Having no geographic factors included in their model, zooplankton are more evenly distributed. Copepods maintain a relatively high density throughout the surface with extreme highs during freshets, seaward movement of brackish water from high river discharge (fig 13). Amphipods have very low densities throughout except for freshets where they reach maximum densities (fig 14).

Time-averaged values of the study area show the aggregation zones for gulls to be at a certain distance near all coasts while high murre and amphipod densities are found in the northern portion of the map (fig 11-12, 14). Interestingly, copepod aggregation zones are found near coasts, particularly on southern coasts or bays (fig 13). These observed distributions are true for both before and after the fall transition, with an area decrease 8%, 63%, 71%, and 71% of for the after groups of the gulls, murres, copepods, and amphipods, respectively (table 6).

4. Discussion

4.1. Oceanographic factors and model validity

The difference in means in the southernmost zones imply that there may be more factors at play in the marine end member locations of the study area at least for the marine birds. But overall, the well-replicated means for ten out of twelve zones point to the potential of this model as a sufficient explanator of population densities for these taxa. Pooled densities for all zones (n = 46) give a higher confidence p-value that is non-significant, i.e., the observed and predicted values are not different. A potential next step for this study is to do a test subset with the zooplankton taxa once the time series has accrued more sample data in the oceanographic stations, but for this study, we relate the relative success of the method for birds to the zooplankton group as well.

The fall and rise of temperature and salinity, respectively, past the fall transition may be due to the diminished impingement of the Fraser River plumes into SJA (Sutherland et al., 2011). As a consequence, the more consistent presence of oceanic waters decreases SST variance as well (fig 4, table 3). Finally, increasing wind speeds may be correlated with the advent of winter storms.

4.2. The relationship of population density to each predictor variable

Glaucous-winged gulls have notable resistance to changes in temperature, which is also seen in others reports where the majority of the Salish Sea population overwinter locally (Domalik et al., 2021; Hall, 2022). The rest of the taxa increased in density with warmer temperatures. This is attributed to the high correlation between SST and phytoplankton biomass (R^2 = 0.86). The correlation between SST and phytoplankton may be due to insolation-related increases in temperature, nutrient co-occurrences with temperature with regards to the Fraser River, or an interplay of both. Temperature also has direct positive effects to zooplankton grazing and biomass (Lewandowska et al., 2014) which has cascading effects up the trophic levels.

Density maxima in the 30-psu range for zooplankton may indicate that slightly estuarine conditions are optimal for growth. These maxima may represent the lower salinity limit of marine copepod species which involves the balance of a high salinity habitat with the relatively high nutrients that fresher waters provide (Harrison et al., 1991). Alternatively, the occasional seaward movement of the estuarine plume may introduce and increase populations of estuarine copepod species to the study area (Breckenridge et al., 2020). Meanwhile, the zooplankton TSD curve shows a preference to uniform temperatures, which implies that the mixing that entrains nutrients from depth (Parsons et al., 1981) may also shuttle zooplankton from the surface, resulting in more primary production but less zooplankton biomass overall. An investigation into fall blooms in the Bering Sea bore no significant relationship between the timings of a bloom and the fall overturn (M. F. Sigler et al., 2014), as the overturn is but one of many factors that cause a fall bloom. It may be that steep topographic gradients or variable temperatures that imbalance the water column for an overturn decreases surface densities until such time that other conditions for a bottom-up biomass resurgence line up and increase overall abundances.

Bird densities have a valley-shaped plot with respect to wind intensity, with dual peaks at the low and high end of wind speeds. Research on bird foraging suggests wind speeds influence the behavior of birds during hunting trips, where stronger winds cause more diving times for Cape gannets *Morus capensis* and periods of weaker winds are preferentially spent drifting on water (Mullers et al., 2009). This principal is also applicable in this study, especially for the diving common murre where the wind effect is more pronounced than for the glaucous-winged gull. Anecdotally, more birds are seen resting on the sea surface during weak wind conditions and more birds are seen flying overhead on gusty days. This may be due to their tendency to exploit high winds to reduce energy expenditure during take-off and flight (Mullers et al., 2009; Thorne et al., 2023).

Depth relationships may be due to their hunting strategies, i.e., diving or non-diving. Common murres are divers that can plunge up to 150-m depths (Hedd et al., 2009) while glaucous-winged gulls are more generalists, i.e., they can hunt on surface waters, intertidal zones, urban areas, and even demonstrate instances of kleptoparasitism (Herbert et al., 2019). The hunting times for murres are therefore most often spent on deeper-water areas (Hedd et al., 2009) while the gulls keep to surface feeding. The distance from shore relationship shows a strong proximity factor for the birds, particularly for the gulls. The optimal distance to coast is 1-1.25 km which is consistent with another study identifying it as 0.6-1.7 km (Domalik et al., 2021).

Topography, here calculated as the standard deviation of depth per 1-km^2, was initially added in to account for the shallow sill (Cattle Pass) located at the end of zone 5 that causes turbulent mixing through gravity flows. Anecdotally, populations aggregate to the flood-side of the sill, i.e., zone 5 has large flocks of birds during flood tide while zone 6 has large flocks during ebb tide. Expectations were that density increases with topography, but results had the opposite outcome. Like in the case of SST standard deviation, it may be that the homogenization of zooplankton population from whole-column mixing may have a larger effect than nutrient entrainment to the surface, at least in the period of days. Topography then will not be a sufficient explanator to the sill effect in this area, and tides may play a larger role than topography. Additionally, since the sequence of marine bird observations is done from zones one to six, and again but with the order reversed, observations for zones five and six are done in quick succession. Therefore, averaging the two observations per zone may not completely dampen tidal signal especially for these zones. It is therefore recommended to add in tides as a factor in future applications of this method.

4.3. Density distribution differences and habitat suitability

The aggregation zones for all taxa apart from the glaucous-winged gulls have been affected by seasonal changes with significant decreases after the fall transition. In addition to having lower mean area coverage, the number of aggregation zones for the after group has less variance than the before group. This is in contrast to the modeled ocean variables that have the same variance for both time groups (fig 4), which means that the consistent low-density values after the fall transition are more attributed to biological and ecological reactions to climate rather than a more constricted range of explanatory variables.

Of all the taxa studied, only glaucous-winged gulls have been predicted to maintain their population after the fall transition. Given their generalist nature, it is unsurprising that the glaucous-winged gulls have a higher affinity to geographic factors such as distance from shore and depth, and

since the fall transition is represented by ocean factors, there were no significant differences in the number of their high-density units for the before and after groups. The strong near-coast high-density band of glaucous-winged gulls is due to the combined effect of the distance from shore factor and depth where they prefer nearshore and shallower areas. Meanwhile, common murres, being specialists that subsist on pelagic forage fish, have a higher sensitivity to temperatures. Much like wind intensity, hunting strategies on these birds depend on temperature, where colder conditions force them to reserve energy stores by limiting flight and foraging times, extending time on the sea surface, and increasing the dive frequency and depth (Burke & Montevecchi, 2018). Colder temperatures also increase energy expenditures for these activities (Croll & McLaren, 1993), so the lower temperatures after the fall transition would have an incrementally detrimental impact on foraging efforts. The high-density patch of murres on the northern part of the study area then is linked to the relatively high temperature Fraser River pulses in SJA.

On the other hand, zooplankton are much more susceptible to oceanographic factors. With the time scale of this study, hydrologic transport of estuarine copepods to the study area by the Fraser River is the favored explanation for the increase in zooplankton density during freshets, as compared to the biological response of population growth which takes considerably longer time periods. Aggregation zones for copepods are found adjacent to shorelines despite the lack of the distance from shore factor in their model. This may be due to the interaction of ocean currents around island topography (island wake effects) that merits further investigation.

To determine whether groups with decreased aggregation is a result of fewer population or a more evenly distributed population, total abundances were calculated by getting the sum of all spatial units per day. These are then compared using a paired t-test (fig 15) to see if any significant changes have occurred as fall progressed. Only the common murre and the copepods have non-significant *p*-values which suggests the same abundances around the fall transition period. This would imply that the common murres and copepods are more dispersed such that their densities fall below the threshold of aggregation zones. This falls in line with the empirical relationship between zooplankton density and TSD, topography, where more mixing results in decreased densities due to homogenization across the water column. Wind also has a notably large influence on copepods (table 5) and the observed increase in wind strength post-fall transition serves to deepen the mixed layer depth and dilute the copepod population. Consequently, this affects the distribution of upper trophic levels linked to zooplankton as prey, including marine birds. Amphipods, on the other hand, have smaller aggregation zones as a result of diminished abundances ($p = 0.0178$), as this group already had consistent low aggregation zone counts before the fall transition.

Much of the variability for SST and salinity comes from the Fraser River. This includes ranges not observed in the transect area, and these are ranges which are more favored by the taxa studied, particularly the common murre and the amphipods (fig 12, 14). The frequency of brackish water invasion to SJA is diminished approaching winter owing to decreased rainfall (Rapaport, 2024), which consequently lowers the densities of zooplankton and the common murre. Overall, the fall transition's main reactant, the Fraser River, in combination with the geography and climate, shape how these organisms are distributed in the San Juan islands. The less drastic drops in density for the birds, especially the glaucous-winged gulls, may be due to the more advanced regulatory and adaptive mechanisms to combat changes in climate than zooplankton. In addition to physiological responses, marine birds can also physically move out of the system if conditions are unsuitable for them whereas zooplankton are essentially tied to ocean physics.

5. Future directions

The PEF database contains many more marine bird, mammal, and zooplankton taxa that are continuously updated every year. The methods detailed in this paper should generally be applicable to other taxa in that database as well. One notable limitation that arose is the relatively low dataset for zooplankton which resulted in no test subset being done. This should be corrected once the PEF zooplankton database has grown much more. Another limitation was the lower capacity of the model to explain densities in zones five and six. We hypothesize that tides greatly influence this region and should be added in as a factor or have its effects more efficiently filtered out. If tides are to be added in, then then its synergistic effect with topography may need to be investigated some more. Defining the extent to which this model could be extrapolated outside the San Juan Archipelago would also be a worthwhile endeavor. To that point, future studies could make use of areas closer to the Fraser River to see how populations change in more estuarine environments, as the transect data in San Juan Channel contain only a limited range of estuarine SST and salinity values.

6. Conclusion

This study defined the relationships between environmental variables and marine bird and zooplankton taxa density of seven years within the San Juan Channel and used those relationships to extrapolate predicted density values to SJA. The decline in high-density areas (aggregation zones) in SJA in the one-month window around the fall transition was quantified, with common murres, copepods, and amphipods experiencing drastic decreases while glaucous-winged gulls having negligible changes. Among all the predictors, SST was the most significant overall, having a negative

effect on density as it decreased throughout the fall. For zooplankton, mixing was also significant, as evidenced by the consistent negative relationship between density and the mixing factors topography, TSD, and wind intensity. Apparently, homogenization of zooplankton outweighs nutrient entrainment when it comes to mixing, particularly in non-bloom conditions, diluting zooplankton biomass. We attribute most of the ocean parameter variation in SJA to Fraser River plume fluctuations, with high temperature, low salinity, and high TSD signals from the plume diminishing after the fall transition as it shifts northward and away from the archipelago, resulting in more consistent marine waters in the study area. Monitoring changes to viable representatives of near end-member trophic levels is vital to understand ecosystem shifts in SJA as it experiences seasonal change to give more informed decisions on policy and conservation.

7. Acknowledgements

I offer my heartfelt gratitude to all the people I met in Friday Harbor Laboratories, especially to Dr. Mike Sigler who was immensely impactful to this research even through Google Meet and Zoom screens, to Dr. Alex Marquez and Dr. Rebecca Guenther who were always within reach and who helped keep my progress at a steady pace, and to Dr. Matt Baker and Dr. Jan Newton who always gave grounding and welcome insight. To my PEF peers who contributed in every and all ways: Madeline Baird, Meghana Binraj, Rebecca Breuel, Valerie Culis, Michaela Dean, Celeste Jerome, Lana Rosie Kuo, Alec Leonetti, Maria Pagliaro, Chyenne Pomeroy, Emily Anne Smith, and Kylie West, there's not a version of this paper without you in it. This paper also acknowledges Kristy Kull and Eric Loss for keeping a steady hand on *R/V Kittiwake*, Maia Kreis who guided us here and all the way through, Dr. Parker MacCready for his support on the LiveOcean dataset, and the entire FHL staff. Maraming salamat!

8. References

Ainley, D. G., Spear, L. B., Allen, S. G., & Ribic, C. A. (1996). Temporal and Spatial Patterns in the Diet of the Common Murre in California Waters. *The Condor*, *98*(4), 691–705. https://doi.org/10.2307/1369852

Bakun, A., & Nelson, C. S. (1991). The Seasonal Cycle of Wind-Stress Curl in Subtropical Eastern Boundary Current Regions. *Journal of Physical Oceanography*, *21*(12), 1815–1834. https://doi.org/10.1175/1520-0485(1991)021<1815:TSCOWS>2.0.CO;2

Blight, L. K., Drever, M. C., & Arcese, P. (2015). A century of change in Glaucous-winged Gull (*Larus glaucescens*) populations in a dynamic coastal environment. *The Condor*, *117*(1), 108–120. https://doi.org/10.1650/CONDOR-14-113.1

Boyd, P. W., Collins, S., Dupont, S., Fabricius, K., Gattuso, J., Havenhand, J., Hutchins, D. A., Riebesell, U., Rintoul, M. S., Vichi, M., Biswas, H., Ciotti, A., Gao, K., Gehlen, M., Hurd, C. L., Kurihara, H., McGraw, C. M., Navarro, J. M., Nilsson, G. E., … Pörtner, H. (2018). Experimental strategies to assess the biological ramifications of multiple drivers of global ocean change—A review. *Global Change Biology*, *24*(6), 2239–2261. https://doi.org/10.1111/gcb.14102

Breckenridge, J., Pakhomov, E., Emry, S., & Mahara, N. (2020). Copepod Assemblage Dynamics in a Snowmelt-Dominated Estuary. *Estuaries and Coasts*, *43*(6), 1502–1518. https://doi.org/10.1007/s12237-020-00722-3

Burke, C. M., & Montevecchi, W. A. (2018). Taking the Bite Out of Winter: Common Murres (Uria aalge) Push Their Dive Limits to Surmount Energy Constraints. *Frontiers in Marine Science*, *5*, 63. https://doi.org/10.3389/fmars.2018.00063

Carrington, E., Roberts, E. A., & Leuchtenberger, S. G. (2022). *Weather Station data from University of Washington Friday Harbor Laboratories, Friday Harbor WA, Cantilever Point from 2006 to 2021* (Version 3) [Dataset]. Biological and Chemical Oceanography Data Management Office (BCO-DMO). https://doi.org/10.26008/1912/BCO-DMO.491262.3

Cox, A. (2021). Physical Oceanographic Conditions Drive Patterns of Seasonal Core Habitat Among Marine Top Predators in the San Juan Archipelago. *Friday Harbor Laboratories*, *Pelagic Ecosystem Function*. http://hdl.handle.net/1773/48603

Croll, D. A., & McLaren, E. (1993). Diving metabolism and thermoregulation in common and thick-billed murres. *Journal of Comparative Physiology B*, *163*(2). https://doi.org/10.1007/BF00263602

Domalik, A. D., Maftei, M., Wright, K. G., Hudson (Trefry), S. A., & Hipfner, J. M. (2021). Migration and Winter Habitat Use of Glaucous-Winged Gulls (Larus glaucescens) from Triangle Island, British Columbia. *Waterbirds*, *44*(4). https://doi.org/10.1675/063.044.0405

Don, C. (2002). Could the San Juan Islands National Wildlife Refuge Serve to Protect Marine Areas? Building on Existing Institutions and Legal Authorities to Create Marine Protected Areas. *Coastal Management*, *30*(4), 421–426. https://doi.org/10.1080/089207502900318

Evans, K., & Kennedy, J. (2007). San Juan County Marine Stewardship Area Plan. *San Juan County Marine Resources Committee*.

Gillman, S. (2021). Predicting at-sea habitat suitability of Alcids in the San Juan Islands, Washington. *Friday Harbor Laboratories*, *Pelagic Ecosystem Function*. http://hdl.handle.net/1773/47172

Hall, H. (2022). *The movement ecology and physiological health of glaucous-winged gulls wintering in the Salish Sea* [M.Sc.]. Simon Fraser University.

Harrison, P., Clifford, P., Cochlan, W., Yin, K., StJohn, M., Thompson, P., Sibbald, M., & Albright, L. (1991). Nutrient and plankton dynamics in the Fraser River plume, Strait of Georgia, British Columbia. *Marine Ecology Progress Series*, *70*, 291–304. https://doi.org/10.3354/meps070291

Hedd, A., Regular, P. M., Montevecchi, W. A., Buren, A. D., Burke, C. M., & Fifield, D. A. (2009). Going deep: Common murres dive into frigid water for aggregated, persistent and slow-moving capelin. *Marine Biology*, *156*(4), 741–751. https://doi.org/10.1007/s00227-008-1125-6

Herbert, S. S., Hayes, F. E., & Hellie, M. E. (2019). Kleptoparasitism of the sea otter (Enhydra lutris) and Steller sea lion (Eumetopias jubatus) by the glaucous-winged gull (Larus glaucescens) at Seward, Alaska. *Polar Biology*, *42*(10), 1935–1941. https://doi.org/10.1007/s00300-019-02559-4

Irons, D. B., Anthony, R. G., & Estes, J. A. (1986). Foraging Strategies of Glaucous-Winged Gulls in a Rocky Intertidal Community. *Ecology*, *67*(6), 1460–1474. https://doi.org/10.2307/1939077

Jacox, M. G., Edwards, C. A., Hazen, E. L., & Bograd, S. J. (2018). Coastal Upwelling Revisited: Ekman, Bakun, and Improved Upwelling Indices for the U.S. West Coast. *Journal of Geophysical Research: Oceans*, *123*(10), 7332–7350. https://doi.org/10.1029/2018JC014187

Lewandowska, A. M., Hillebrand, H., Lengfellner, K., & Sommer, U. (2014). Temperature effects on phytoplankton diversity—The zooplankton link. *Journal of Sea Research*, *85*, 359–364. https://doi.org/10.1016/j.seares.2013.07.003

Loredo, S. (2018). *Movement, dive behavior, and habitat-use of common murres (Uria aalge) in the Northern California Current System under variable ocean conditions. Corvallis, Oregon* [MS]. Oregon State University.

MacCready, P., McCabe, R. M., Siedlecki, S. A., Lorenz, M., Giddings, S. N., Bos, J., Albertson, S., Banas, N. S., & Garnier, S. (2021). Estuarine Circulation, Mixing, and Residence Times in the Salish Sea. *Journal of Geophysical Research: Oceans*, *126*(2), e2020JC016738. https://doi.org/10.1029/2020JC016738

Mullers, R., Navarro, R., Daan, S., Tinbergen, J., & Meijer, H. (2009). Energetic costs of foraging in breeding Cape gannets Morus capensis. *Marine Ecology Progress Series*, *393*, 161–171. https://doi.org/10.3354/meps08250

NOAA National Geophysical Data Center. (2003). *U.S. Coastal Relief Model Vol.8—Northwest Pacific* [Dataset]. NOAA National Centers for Environmental Information. https://doi.org/10.7289/V5H12ZXJ

Parsons, T., Stronach, J., Borstad, G., Louttit, G., & Perry, R. (1981). Biological Fronts in the Strait of Georgia, British Columbia, and Their Relation to Recent Measurements of Primary Productivity. *Marine Ecology Progress Series*, *6*, 237–242. https://doi.org/10.3354/meps006237

Pawlowicz, R., Riche, O., & Halverson, M. (2007). The circulation and residence time of the strait of Georgia using a simple mixing-box approach. *Atmosphere-Ocean*, *45*(4), 173–193. https://doi.org/10.3137/ao.450401

Perry, R. I., Young, K., Galbraith, M., Chandler, P., Velez-Espino, A., & Baillie, S. (2021). Zooplankton variability in the Strait of Georgia, Canada, and relationships with the marine survivals of Chinook and Coho salmon. *PLOS ONE*, *16*(1), e0245941. https://doi.org/10.1371/journal.pone.0245941

R Core Team. (2024). *R: A Language and Environment for Statistical Computing* [Computer software]. R Foundation for Statistical Computing. https://www.R-project.org/

Rapaport, M. (Ed.). (2024). *Salish Archipelago: Environment and Society in the Islands Within and Adjacent to the Salish Sea* (1st ed.). ANU Press. https://doi.org/10.22459/SA.2024

Reid, W. V. (1988). Population dynamics of the glaucous-winged gull. *The Journal of Wildlife Management*, *52*(4), 763–770.

Sigler, M. F., Stabeno, P. J., Eisner, L. B., Napp, J. M., & Mueter, F. J. (2014). Spring and fall phytoplankton blooms in a productive subarctic ecosystem, the eastern Bering Sea, during 1995–2011. *Deep Sea Research Part II: Topical Studies in Oceanography*, *109*, 71–83. https://doi.org/10.1016/j.dsr2.2013.12.007

Sigler, M., Rooper, C., Goddard, P., Wilborn, R., & Williams, K. (2023). Alaska deep-sea coral and sponge assemblages are well-defined and mostly predictable from local environmental conditions. *Marine Ecology Progress Series*, *712*, 67–85. https://doi.org/10.3354/meps14317

Steinberg, D. K., Carlson, C. A., Bates, N. R., Goldthwait, S. A., Madin, L. P., & Michaels, A. F. (2000). Zooplankton vertical migration and the active transport of dissolved organic and inorganic carbon in the Sargasso Sea. *Deep Sea Research Part I: Oceanographic Research Papers*, *47*(1), 137–158. https://doi.org/10.1016/S0967-0637(99)00052-7

Sutherland, D. A., MacCready, P., Banas, N. S., & Smedstad, L. F. (2011). A Model Study of the Salish Sea Estuarine Circulation*. *Journal of Physical Oceanography*, *41*(6), 1125–1143. https://doi.org/10.1175/2011JPO4540.1

The MathWorks Inc. (2024). *MATLAB* (Version 23.2.0.2485118 (R2023b)) [Computer software]. The MathWorks Inc. https://www.mathworks.com

Thomson, R. E., Kulikov, E. A., Spear, D. J., Johannessen, S. C., & Peter Wills, W. (2020). A Role for Gravity Currents in Cross-Sill Estuarine Exchange and Subsurface Inflow to the Southern Strait of Georgia. *Journal of Geophysical Research: Oceans*, *125*(4), e2019JC015374. https://doi.org/10.1029/2019JC015374

Thorne, L., Clay, T., Phillips, R., Silvers, L., & Wakefield, E. (2023). Effects of wind on the movement, behavior, energetics, and life history of seabirds. *Marine Ecology Progress Series*, *723*, 73–117. https://doi.org/10.3354/meps14417

Wood, S. N. (2011). Fast Stable Restricted Maximum Likelihood and Marginal Likelihood Estimation of Semiparametric Generalized Linear Models. *Journal of the Royal Statistical Society Series B: Statistical Methodology*, *73*(1), 3–36. https://doi.org/10.1111/j.1467-9868.2010.00749.x

Zamon, J. (2003). Mixed species aggregations feeding upon herring and sandlance schools in a nearshore archipelago depend on flooding tidal currents. *Marine Ecology Progress Series*, *261*, 243–255. https://doi.org/10.3354/meps261243

10. List of figures and tables

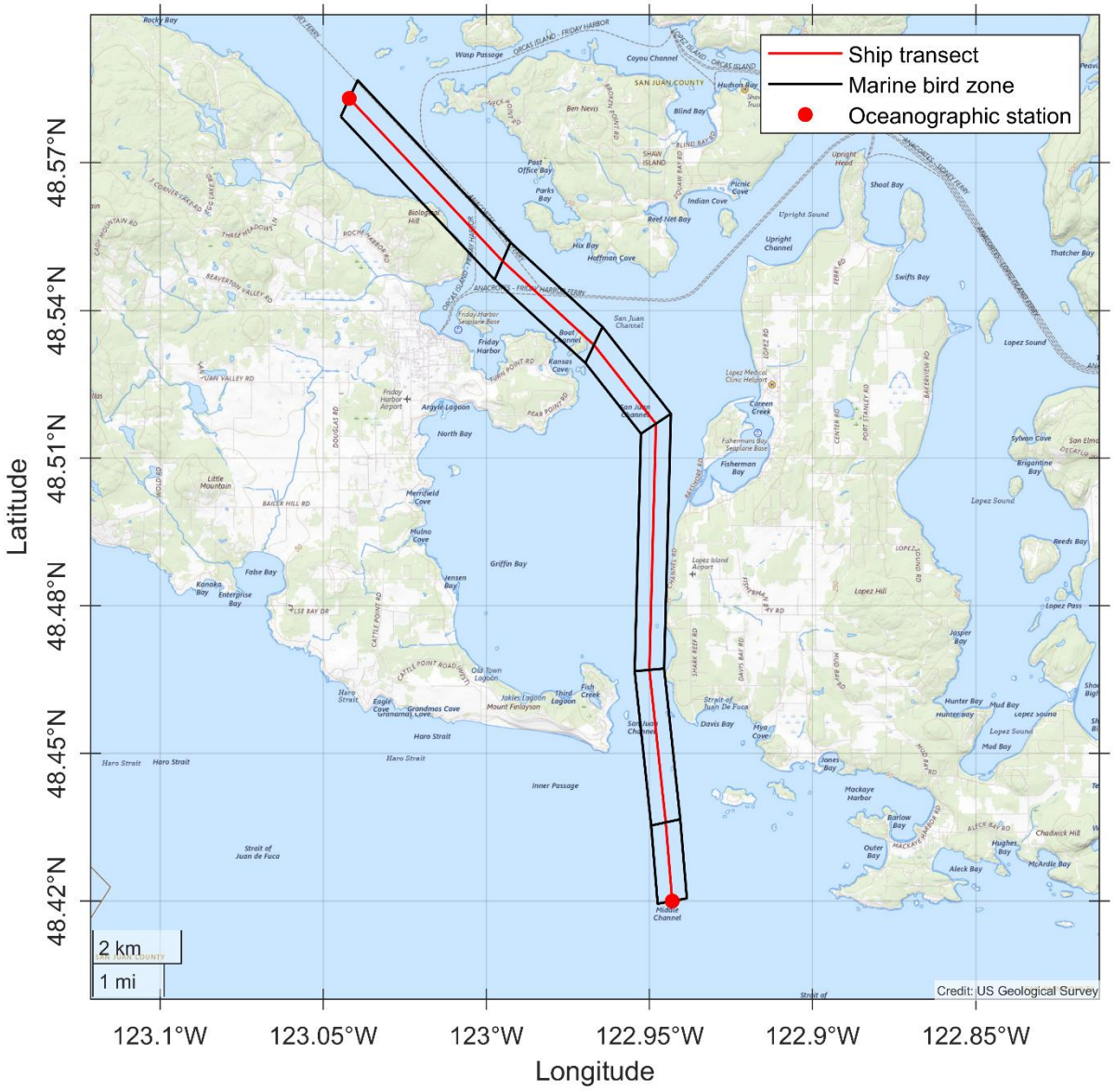

Figure 1. Survey area for oceanography and marine birds. Red line delineates the approximate ship transect route. Black polygons centered around the transect represent zones 1-6 from north to south. The width of each zone is about 500 meters on each side of the transect. Red dots on the top and bottom ends mark the North and South stations, respectively.

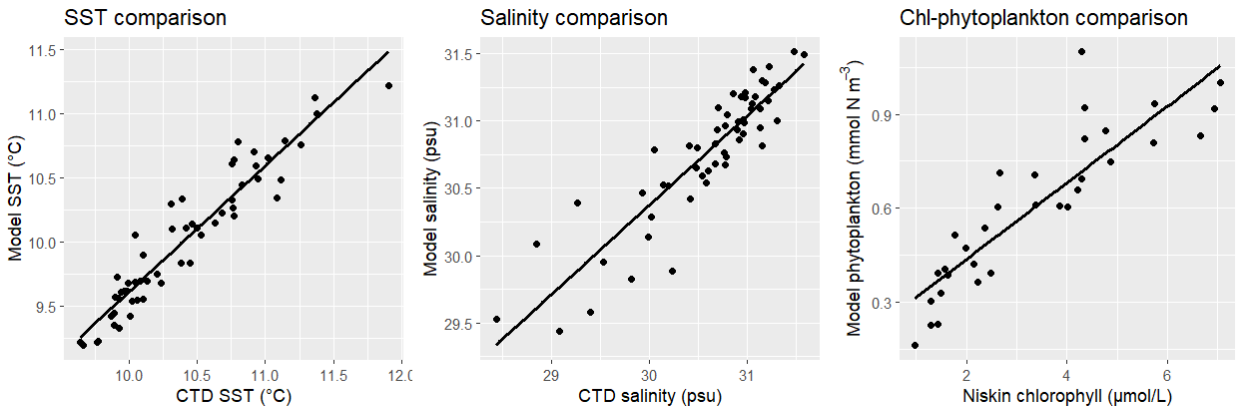

Figure 2. Comparisons between observed and model values for SST, surface salinity, and chlorophyll (discrete) and phytoplankton (model). The black line is the linear regression fitted line.

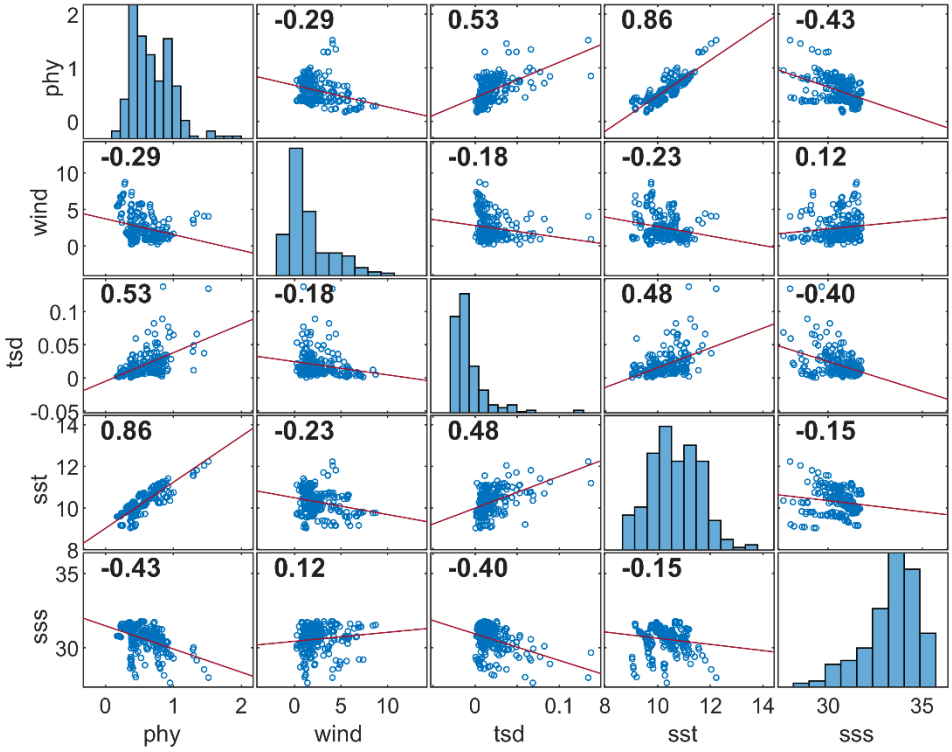

Figure 3. Correlation matrix of dynamic variables during cruise dates within all zones. Numeric values on the regression plots show R^2 values.

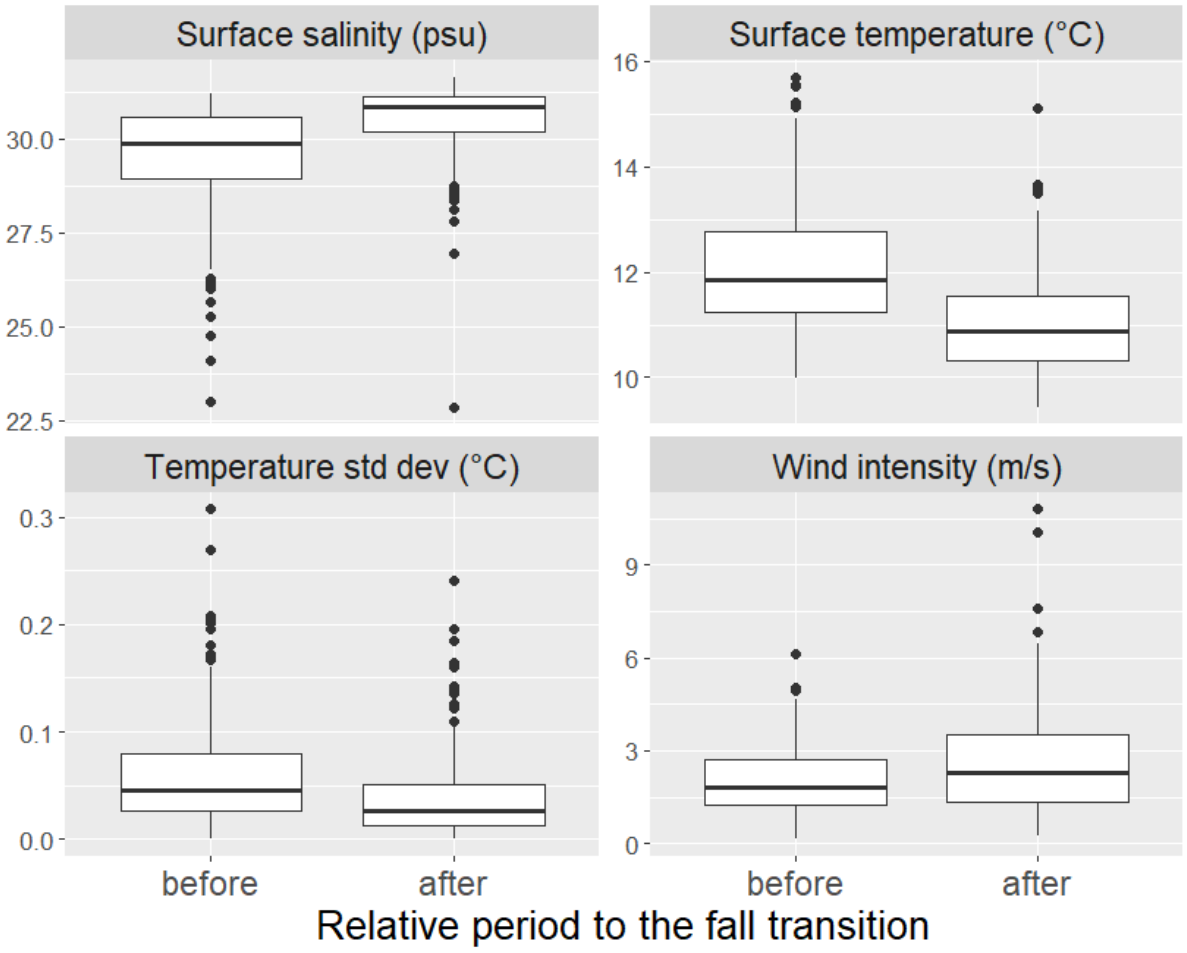

Figure 4. Box plots for sea surface temperature, salinity, temperature standard deviation, and wind speed before and after the fall transition. All *p*-values < 0.001.

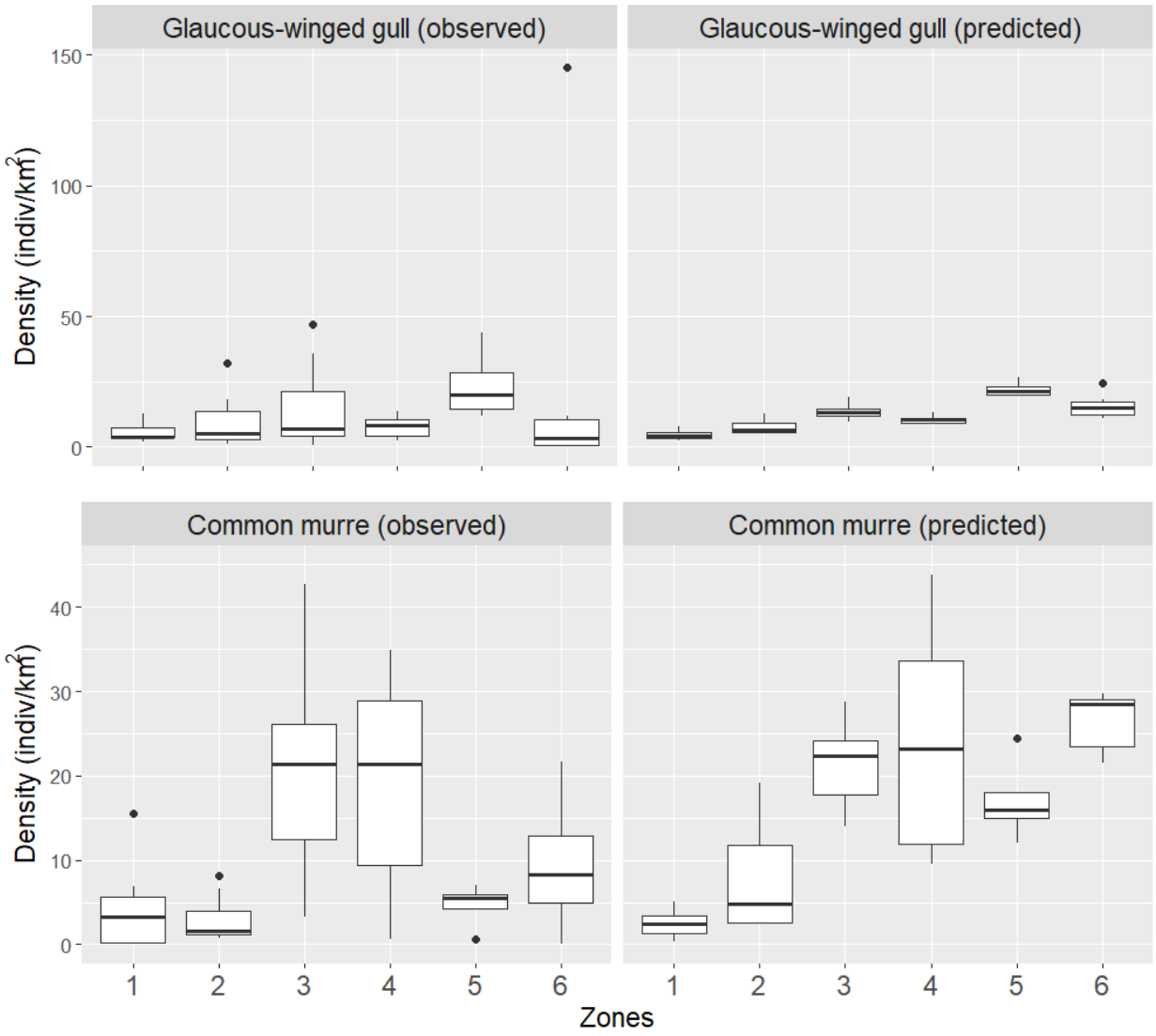

Figure 5. Comparison of mean densities by zone of observed (left column) and predicted values (right column) for glaucous-winged gulls (top row) and common murres (bottom row).

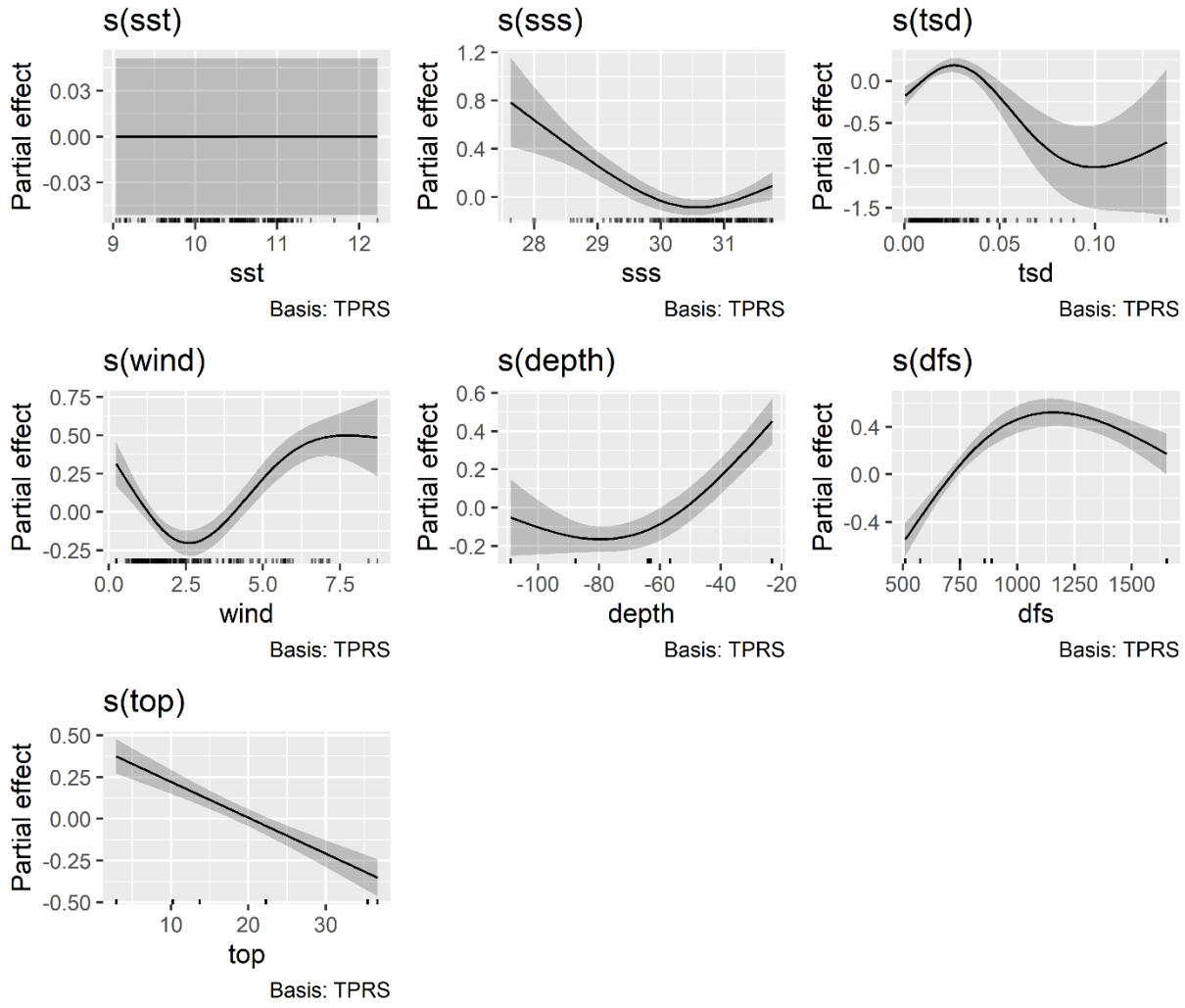

Figure 6. Generalized additive model results for the glaucous-winged gull; sst – sea surface temperature, sss – sea surface salinity, tsd – temperature standard deviation, wind – wind speed, dfs – distance from shore, top – topography. The horizontal line for sst implies that this factor is non-significant.

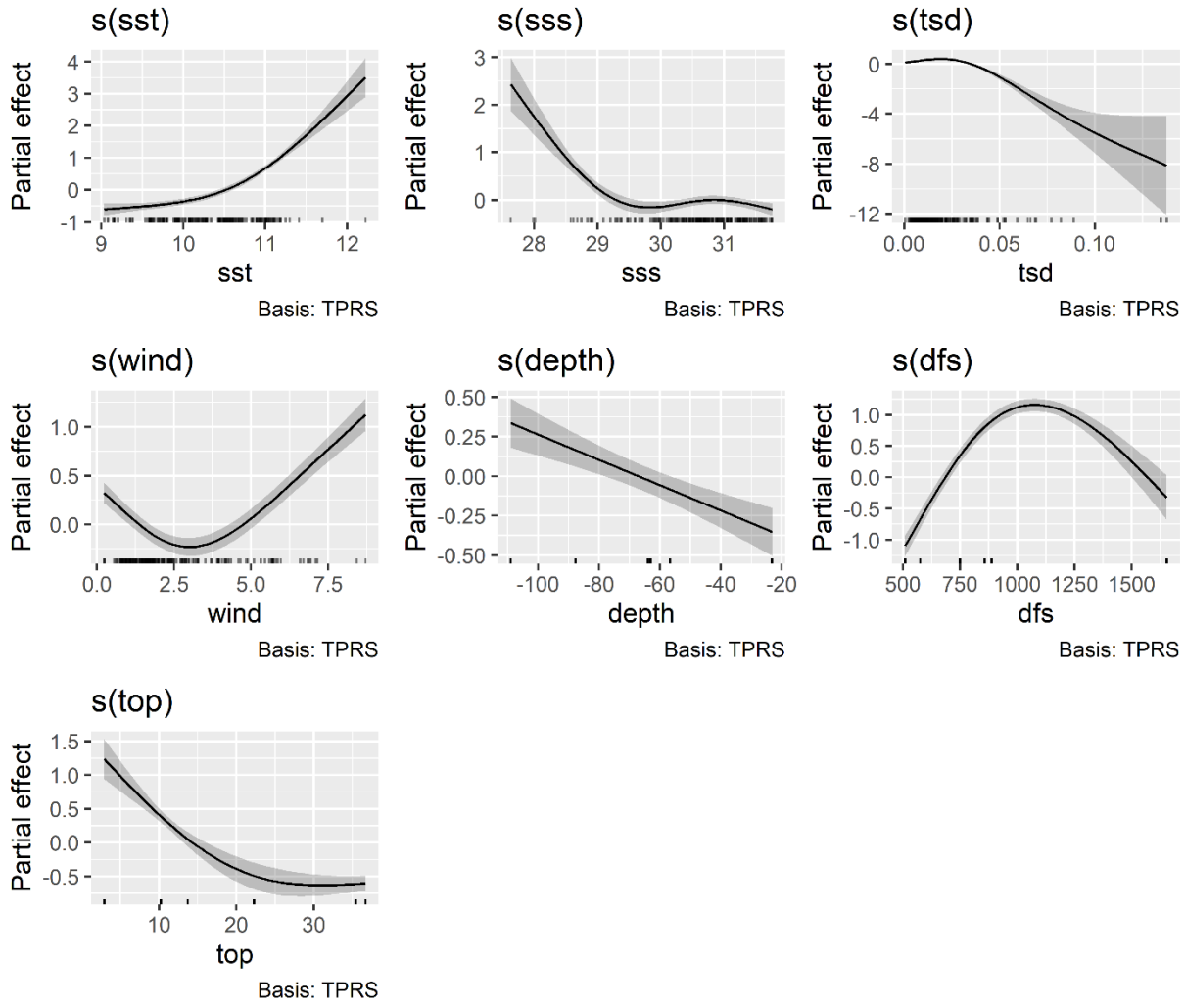

Figure 7. Generalized additive model results for the common murre; sst – sea surface temperature, sss – sea surface salinity, tsd – temperature standard deviation, wind – wind speed, dfs – distance from shore, top – topography.

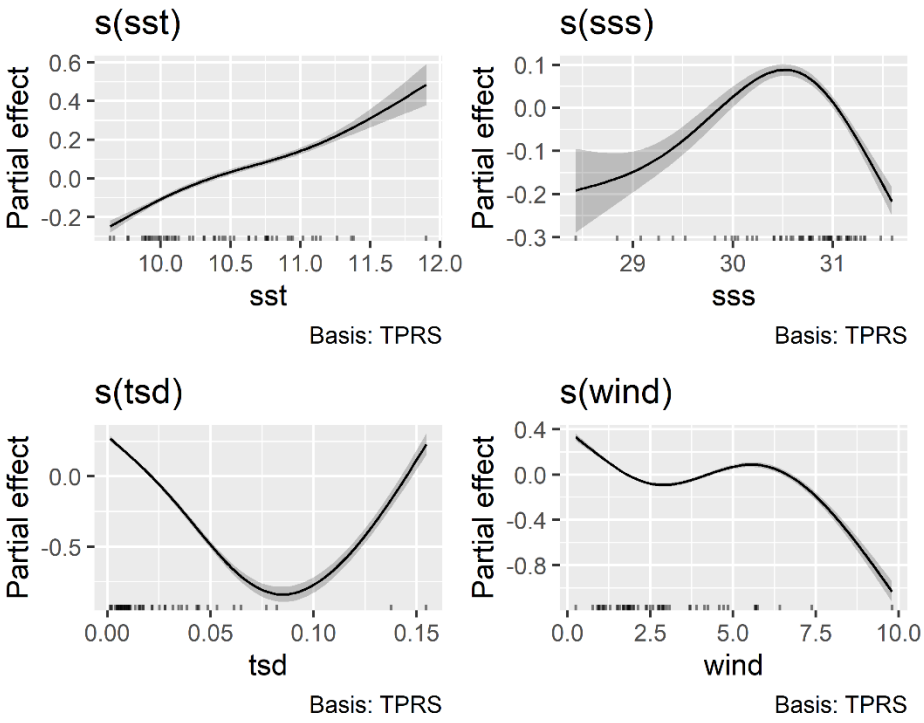

Figure 8. Generalized additive model results for copepods; sst – sea surface temperature, sss – sea surface salinity, tsd – temperature standard deviation, wind – wind speed, dfs – distance from shore, top – topography.

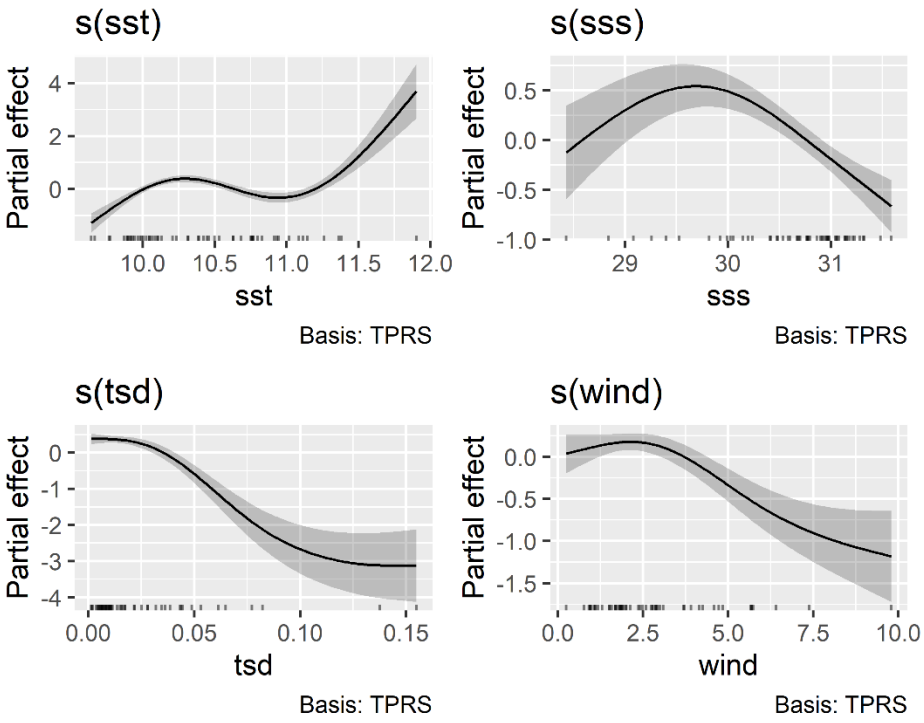

Figure 9. Generalized additive model results for amphipods; sst – sea surface temperature, sss – sea surface salinity, tsd – temperature standard deviation, wind – wind speed, dfs – distance from shore, top – topography.

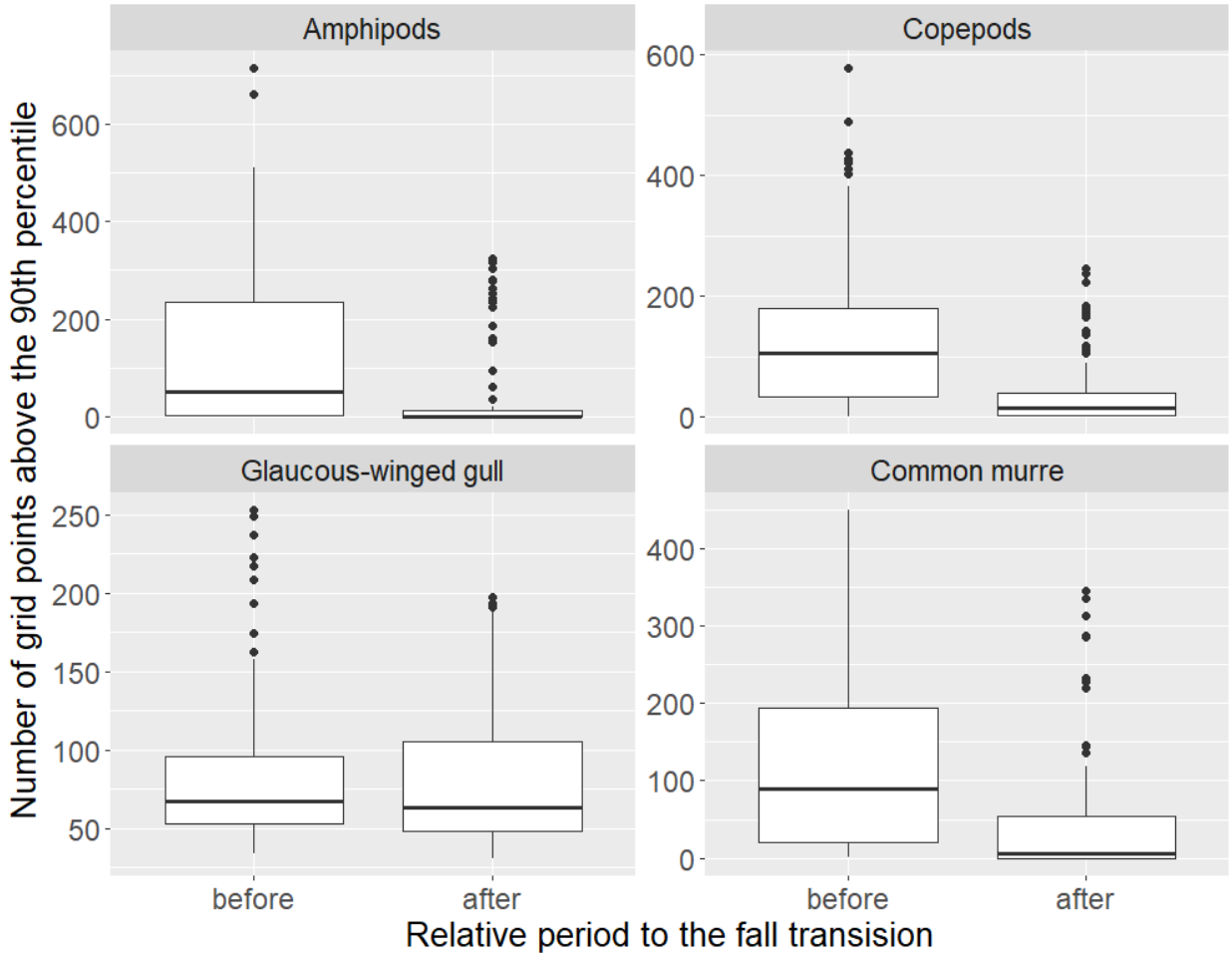

Figure 10. Comparison of number of grid points above the 90th percentile of before and after the fall transition for each taxon.

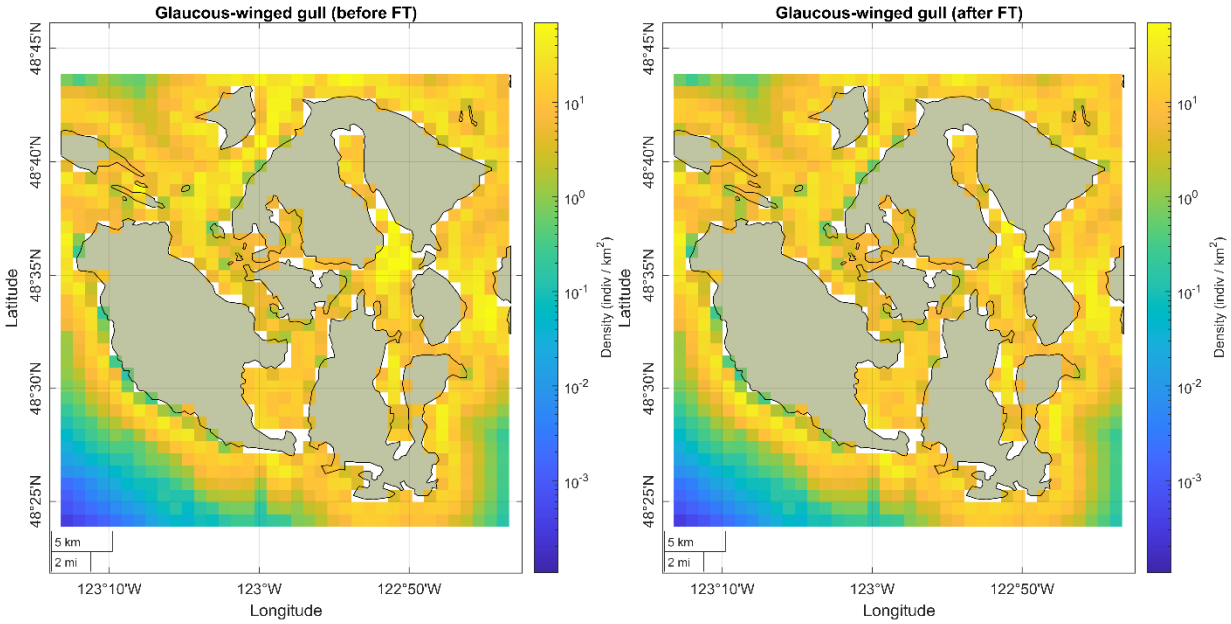

Figure 11. Mean density values of glaucous-winged gulls grouped by relative time to the fall transition (before and after).

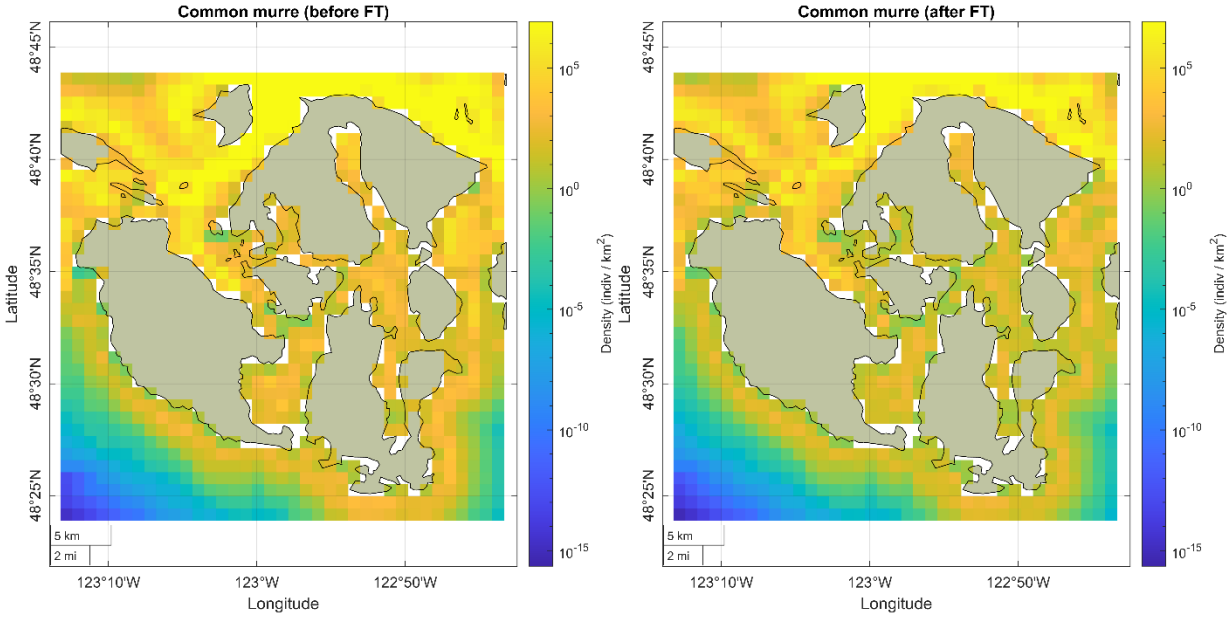

Figure 12. Mean density values of common murres grouped by relative time to the fall transition (before and after).

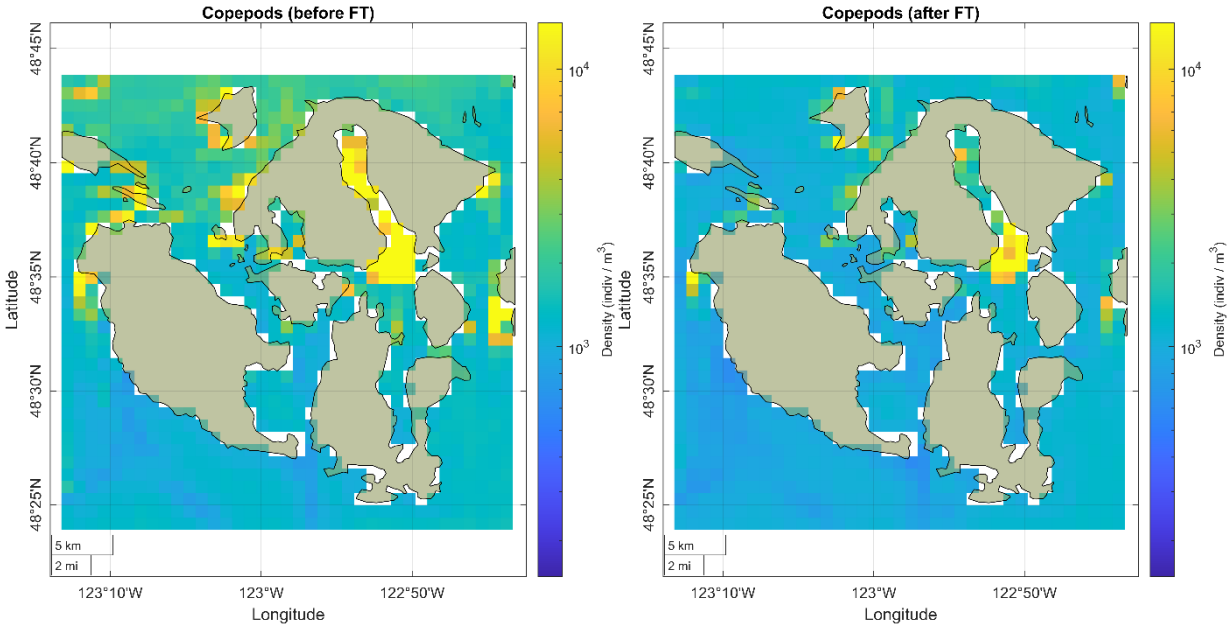

Figure 13. Mean density values of copepods grouped by relative time to the fall transition (before and after).

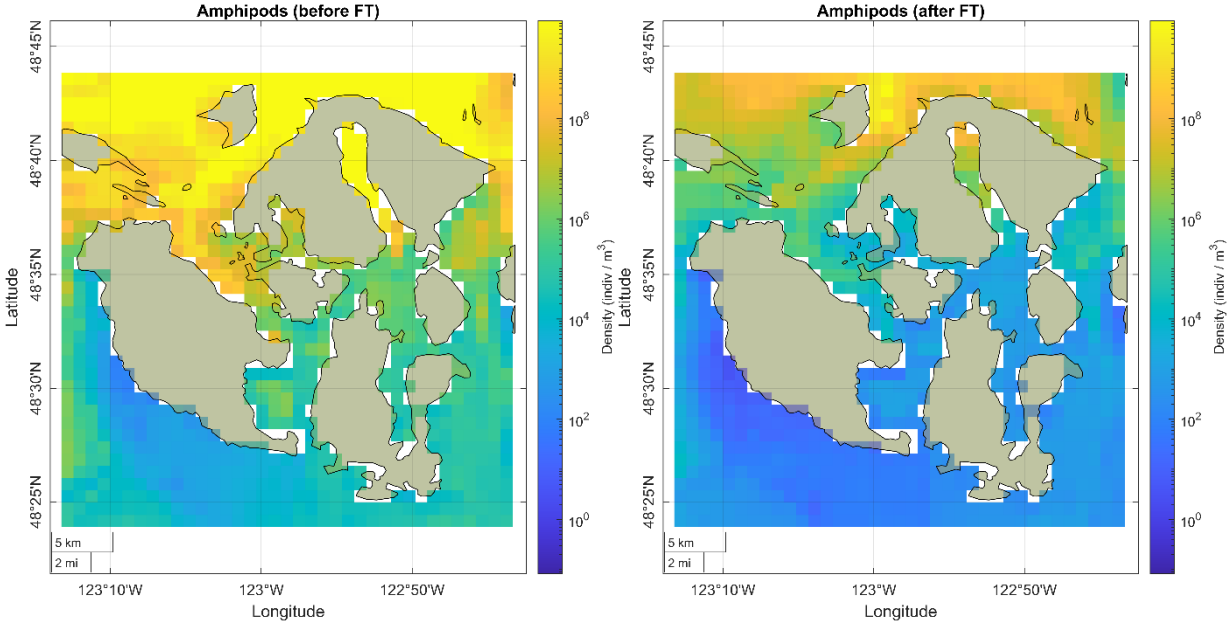

Figure 14. Mean density values of amphipods grouped by relative time to the fall transition (before and after).

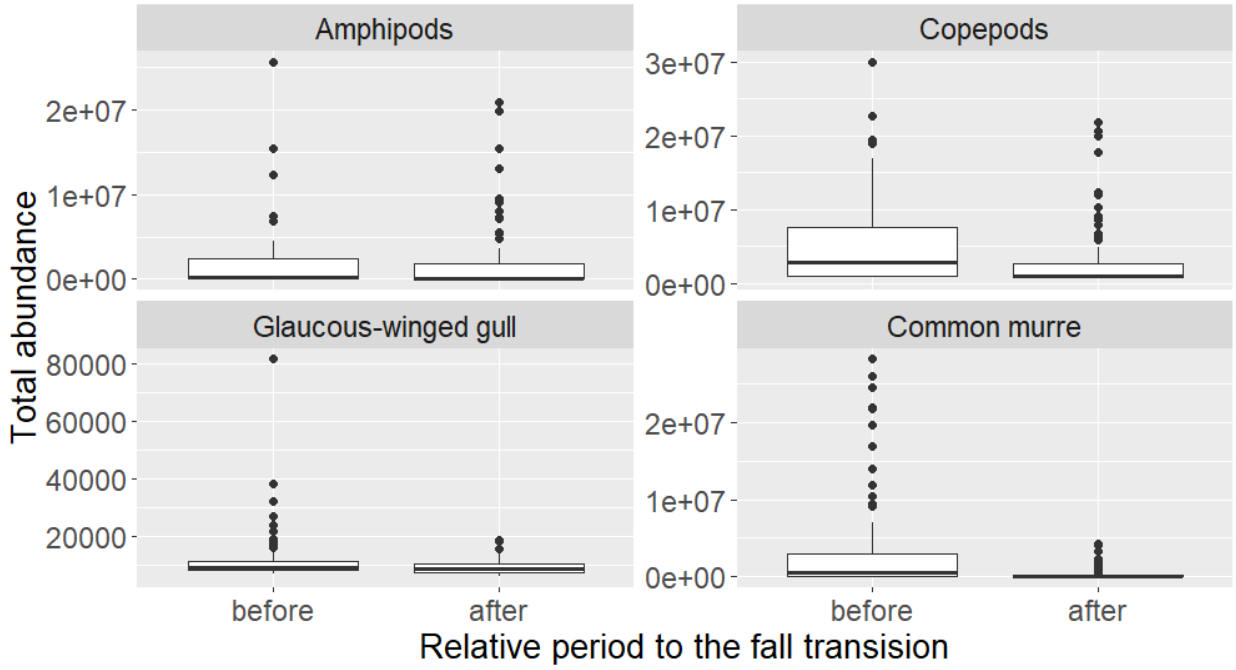

Figure 15. Comparison of total abundances of the study area. Data points beyond Q1 and Q3 by 1.5 times the interquartile range are not displayed but are included in calculations for table 7 for readability.

Station/Zone	North endpoint (°)	South endpoint (°)	Length (km)	Area (km^2)
North	48.583, -123.042		-	-
1	48.583, -123.042	48.550, -122.995	5.05	2.020
2	48.550, -122.995	48.533, -122.967	2.80	1.120
3	48.533, -122.967	48.517, -122.948	2.27	0.908
4	48.517, -122.948	48.467, -122.950	5.56	2.224
5	48.467, -122.950	48.433, -122.945	3.80	1.520
6	48.433, -122.945	48.420, -122.943	1.45	0.580
South	48.420, -122.943		-	-

Table 1. Geographic information for the zones and stations.

Regression variable	Surface temperature	Surface salinity	Chlorophyll (discrete) vs phytoplankton (model)
Intercept	-0.2304	10.5198	0.1929
Slope	0.9839	0.6618	0.1221
R^2	0.8980	0.8031	0.7694

Table 2. Regression values for observed vs modeled SST, surface salinity, and chlorophyll (discrete) and phytoplankton (model).

Variable	Max	Min	Mean before	Mean after	*t*-test *p*-value	Difference (after – before)
SST (°C)	16.44	9.28	12.13	11.03	4.341e-15	−1.10373 °C
Surface salinity (psu)	31.82	21.19	29.48	30.48	3.565e-10	1.00455 psu
Temperature standard deviation (°C)	0.97	0	0.060	0.039	0.0004572	−0.02091982 °C
Wind intensity (m/s)	11.35	0.01	2.026	2.678	0.0003441	0.651996 m/s

Table 3. Paired t-test p-values for dynamic variable comparisons for before and after the fall transition. Max and min columns refer to the total dataset irrespective of whether it is before or after the fall transition.

Zone	*p*-value (glaucous-winged gull)	*p*-value (common murre)
1	0.4387	0.4063
2	0.5334	0.0840
3	0.8831	0.2836
4	0.2331	0.5640
5	0.8101	0.4732
6	0.6779	0.4949
All	0.5481	0.7662

Table 4. List of *p*-values for the correlation between observed and predicted densities of each zone for glaucous-winged gull and common murre.

	EDF	Chi-square	*p*-value
	Glaucous-winged gull		
SST	0.00	0.00	0.494
SSS	2.21	31.12	1.28E-07
TSD	2.85	27.82	2.55E-06
WIND	2.92	84.55	< 2e-16
DEPTH	1.60	78.49	< 2e-16
DFS	1.95	80.60	< 2e-16
TOP	0.94	56.56	< 2e-16
	Common murre		
SST	2.89	646.77	<2e-16
SSS	2.99	101.23	<2e-16
TSD	2.73	138.98	<2e-16
WIND	1.99	204.06	<2e-16
DEPTH	0.93	26.25	<2e-16
DFS	1.86	563.40	<2e-16
TOP	1.84	245.94	<2e-16
	Copepods		
SST	2.80	669.40	<2e-16
SSS	2.91	281.00	<2e-16
TSD	2.98	1777.30	<2e-16
WIND	3.00	837.40	<2e-16
	Amphipods		
SST	3.00	82.57	<2e-16
SSS	1.86	35.62	<2e-16
TSD	1.97	73.35	<2e-16
WIND	1.88	34.01	<2e-16

Table 5. GAM statistics per predictor for each taxonomic group. SSS = salinity, TSD = temperature standard deviation, DFS = distance from shore, TOP = topography.

	Mean area before FT (km^2)	Mean area after FT (km^2)	Percent decrease (%)	p-value

Glaucous-winged gull	86.02041	79.47959	7.60	0.267
common murre	125.4388	46.06122	63.28	<0.001
Copepods	137.0612	39.2449	71.37	<0.001
Amphipods	136.6837	39.81633	70.87	<0.001

Table 6. Mean area of aggregation zones (1-km^2 grids above the 90th density percentile) before and after the fall transition per taxonomic group.

	Mean total abundance before	**Mean total abundance after**	***p*-value**
Glaucous-winged gull	11799.250	9580.888	0.0178
common murre	3.41e+12	4.45e+10	0.2770
Copepods	1.07e+10	1.64e+7	0.2939
Amphipods	1.52e+13	5.92e+10	0.0135

Table 7. Mean total abundances for each taxon grouped by relative time to the fall transition and *p*-values of the corresponding paired *t*-test.